Spin-Fluctuation Mechanism of Anomalous Temperature Dependence of Magnetocrystalline Anisotropy in Itinerant Magnets

I. A. Zhuravlev,[1] V. P. Antropov,[2] and K. D. Belashchenko[1]
[1]Department of Physics and Astronomy and Nebraska Center for Materials and Nanoscience, University of Nebraska-Lincoln, Lincoln, Nebraska 68588, USA
[2]Ames Laboratory, U.S. Department of Energy, Ames, Iowa 50011, USA
(Received 2 April 2015; published 16 November 2015)

The origins of the anomalous temperature dependence of magnetocrystalline anisotropy in $(Fe_{1-x}Co_x)_2B$ alloys are elucidated using first-principles calculations within the disordered local moment model. Excellent agreement with experimental data is obtained. The anomalies are associated with the changes in band occupations due to Stoner-like band shifts and with the selective suppression of spin-orbit "hot spots" by thermal spin fluctuations. Under certain conditions, the anisotropy can increase, rather than decrease, with decreasing magnetization due to these peculiar electronic mechanisms, which contrast starkly with those assumed in existing models.

DOI: 10.1103/PhysRevLett.115.217201 PACS numbers: 75.30.Gw, 71.23.-k, 75.10.Lp, 75.50.Ww

Magnetocrystalline anisotropy (MCA) is one of the key properties of a magnetic material [1]. Understanding its temperature dependence is a challenging theoretical problem with implications for the design of better materials for permanent magnets [2], heat-assisted magnetic recording [3], and other applications. While the MCA energy K usually declines monotonically with increasing temperature as predicted by simple models [4], in some magnets it behaves very differently and can even increase with temperature. Such anomalous $K(T)$ dependence makes some materials useful as permanent magnets and can potentially facilitate specialized applications.

Well-known anomalies in the temperature dependence of MCA include spin reorientation transitions (SRTs) in cobalt [5] and MnBi [6], which have been attributed to thermal expansion, an SRT in gadolinium, which may be due to higher-order terms in MCA [7], SRTs in $R_2Fe_{14}B$ hard magnets [8] due to the ordering of the rare-earth spins at low T, and SRTs in thin films [9,10] associated with the competition between the bulk and surface contributions to MCA. Competition between single-site and two-site MCA can also lead to a SRT [11].

MCA in metallic magnets is rarely dominated by the single-ion mechanism leading to the $K \propto M^3$ dependence on the magnetization [4]. For example, two-ion terms in $3d$-$5d$ alloys like FePt modify this dependence to $K \propto M^{2.1}$ [12,13]. Clear understanding of the anomalous temperature dependence of MCA has been so far limited to the cases when competing contributions to MCA can be sorted out in real space, such as, for example, bulk and surface terms in thin films. In contrast, understanding of MCA in itinerant magnets usually requires a reciprocal space analysis [14].

One such system is the disordered substitutional $(Fe_{1-x}Co_x)_2B$ alloy, which exhibits three concentration-driven SRTs at $T = 0$, a high-temperature SRT at the Fe-rich end, and a strongly nonmonotonic temperature dependence at the Co-rich end with a low-temperature SRT [15,16]. The SRTs at $T = 0$ were traced down to the variation of the band filling with concentration combined with spin-orbital selection rules [16]. Here we elucidate the unconventional mechanisms leading to the spectacular anomalies in the temperature dependence of MCA in this system and show that they stem from the changes in the electronic structure induced by spin fluctuations. We will see that under certain conditions MCA can increase, rather than decrease, with decreasing magnetization due to these mechanisms.

Our calculations employ the Green's function-based linear muffin-tin orbital method [17] with spin-orbit coupling (SOC) included as a perturbation to the potential parameters [16,18]. Thermal spin fluctuations are included within the disordered local moment (DLM) model [19,20], which treats them within the coherent potential approximation (CPA) on the same footing with chemical disorder. The DLM method has been previously used to calculate the $K(T)$ dependence in systems like FePt [21,22] and YCo_5 [23]. Although $K(T)$ in these metals does not follow the Callen-Callen model [4] designed for materials with single-ion MCA, it still decreases monotonically. In contrast, we will see that the changes in the electronic structure with temperature lead to strong anomalies in $(Fe_{1-x}Co_x)_2B$. Our implementation of the DLM method is described in Ref. [24]. (See Supplemental Material [25] for additional details.)

Apart from the inclusion of spin disorder, the computational details are similar to Ref. [16]. In particular, the large overestimation of the magnetization in density-functional calculations for Co_2B ($1.1\mu_B$ compared to experimental $0.76\mu_B$ per Co atom) is corrected by scaling the local part of the exchange-correlation field for Co atoms by a factor 0.8 at all concentrations. This treatment is consistent with

spin-fluctuation theories showing that spin fluctuations tend to reduce the effective Stoner parameter [36,37] and allows us to take into account the resulting changes in the electronic structure.

Magnetism in $(Fe_{1-x}Co_x)_2B$ alloys is much more itinerant compared to systems like FePt; the spin moments of Fe and, especially, Co atoms are not rigid in density-functional calculations. To implement spin disorder within the DLM method, we make a simple assumption that the spin moments of both Fe and Co at finite T can be taken from the ferromagnetic state at $T = 0$. This assumption is based on the expectation that thermal spin fluctuations to a large extent restore the "soft" spin moments [36]. On the other hand, the variation of the electronic structure with T should not be very sensitive to the details of the spin fluctuation model. For simplicity, a similar approach is used for the $(Co_{1-x}Ni_x)_2B$ system, including the small spin moments on the Ni atoms.

The distribution functions for spin orientations are taken in the Weiss form: $p_\nu(\theta) \propto \exp(\alpha_\nu \cos\theta)$, where θ is the angle made by the spin with the magnetization axis, and ν labels the alloy component. The temperature dependence of the coefficients α_ν is determined using the calculated effective exchange parameters, as explained in the Supplemental Material [25]. Fermi-Dirac smearing is neglected, because the effects of spin fluctuations are overwhelmingly stronger.

The results of $K(x, T)$ calculations shown in Fig. 1, which were obtained with temperature-independent lattice parameters, are in excellent agreement with experimental data [15]. Both the thermal SRT at the Fe-rich end and the nonmonotonic temperature dependence at the Co-rich end in $(Fe_{1-x}Co_x)_2B$ alloys are captured (see Supplemental Material [25] for a direct comparison). For $(Co_{0.9}Ni_{0.1})_2B$ the MCA energy at $T = 0$ is large and negative in agreement with experiment [15], although the initial decline of $K(T)$ similar to Co_2B is not observed in experiment. The finite slope in the $K(T)$ curves at zero temperature is due to the classical treatment of spin fluctuations. We have explicitly verified that the effect of thermal expansion on $K(T)$ in Fe_2B and Co_2B is almost unnoticeable.

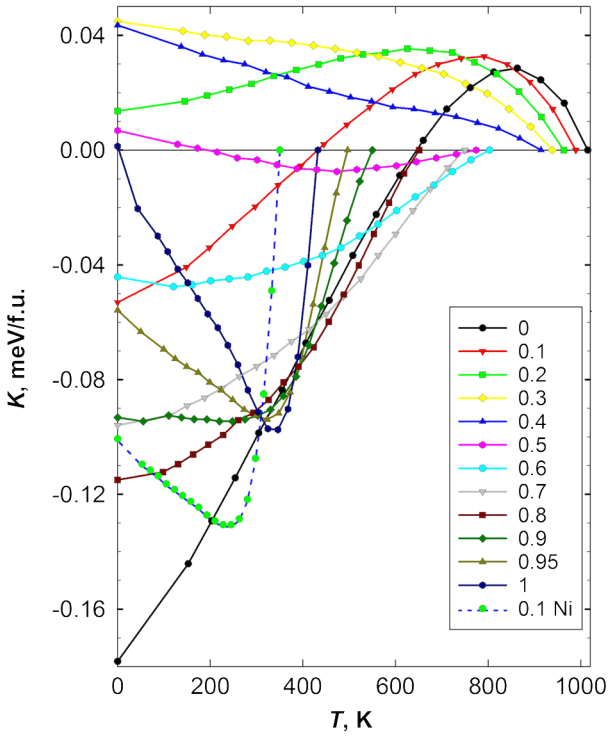

FIG. 1 (color online). Calculated temperature dependencies of MCA energy K in $(Fe_{1-x}Co_x)_2B$ and $(Co_{0.9}Ni_{0.1})_2B$ alloys.

The effects of spin disorder on the electronic structure can be understood from Fig. 2, which shows the partial minority-spin Bloch spectral function at $x = 0.95$ for $T = 0$ and $T/T_C = 0.7$. Here, at the Co-rich end, all bands are easily identifiable and relatively weakly broadened at $T/T_C = 0.7$. In addition, they are shifted down relative to their positions at $T = 0$, which is a hallmark of an itinerant Stoner system. In contrast, at the Fe-rich end the bands are strongly broadened by spin fluctuations, so that most bands

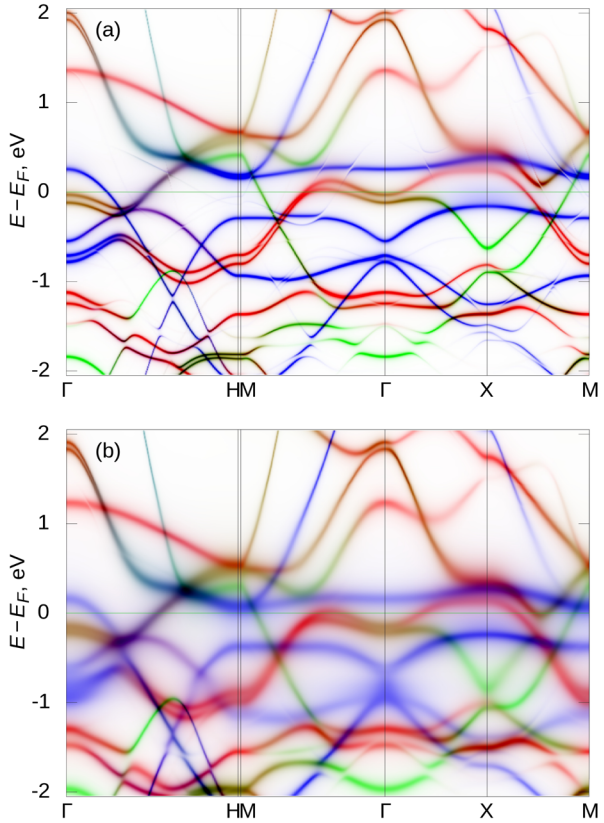

FIG. 2 (color online). Partial minority-spin spectral function for the transition-metal site in $(Fe_{0.05}Co_{0.95})_2B$ at (a) $T = 0$, and (b) $T/T_C = 0.7$. SOC is included, $\mathbf{M}\|z$, and the energy is in eV. Color encodes the orbital character of the states. The intensities of the red, blue, and green color channels are proportional to the sum of $m = \pm 2$ (xy and $x^2 - y^2$), sum of $m = \pm 1$ (xz and yz), and $m = 0$ (z^2) character, respectively.

in the 1 eV window below E_F are barely visible (see Supplemental Material [25]). The large difference in the degree of band broadening between the Fe-rich and Co-rich ends is due to the 2.5-fold difference in the magnitude of the spin moments. The effect of phonon scattering on band broadening in $(Fe_{1-x}Co_x)_2B$ alloys is likely much smaller and is neglected here.

The usual expectation is that spin disorder should reduce MCA as a result of averaging over spin directions. Such normal behavior is seen, for example, at $x = 0.3$ in Fig. 1. This expectation is violated at many concentrations: $K(x,T)$ is nonmonotonic with respect to T at $0 \le x \le 0.2$, $0.5 \le x \le 0.6$, and $0.9 \le x \le 1$; we will call this behavior anomalous. At $x \le 0.6$ the anomalous temperature dependence of K at a given x follows the variation of K with increasing x at $T = 0$. For example, $K(0.2,0) > K(0.1,0)$, and $K(0.1,T)$ anomalously increases with T. At $x \ge 0.9$ the anomalous variation is opposite to the trend in $K(x,0)$ with increasing x. To understand this difference, we first need to examine the effect of disorder on MCA.

Figure 3 compares $K(x,0)$ calculated within the virtual crystal approximation (VCA) with CPA results for $(Fe_{1-x}Co_x)_2B$ [16] and $(Co_{1-x}Ni_x)_2B$ systems [38]. Note that in the $(Co_{1-x}Ni_x)_2B$ system the spin moments vanish near 40% Ni, in agreement with experiment [39]. In addition to the MCA energy K, Fig. 3 also shows its approximate spin decomposition $K_{\sigma\sigma'}$ obtained from the SOC energy [16,25]. Because the $3d$ shell in this system is more than half filled, the variation of MCA with x is largely controlled by the $K_{\downarrow\downarrow}$ term, i.e., by the L_zS_z mixing of the minority-spin states. Substitutional disorder strongly suppresses MCA, an effect that was also found in tetragonal Fe-Co alloys [40]. The suppression is due to band broadening, which reduces the efficiency of spin-orbital selection rules. Importantly, bands broaden at different rates; the contributions to MCA from the bands that lie close to E_F and broaden strongly are most effectively suppressed. The dispersive majority-spin bands are weakly broadened, and hence the $K_{\uparrow\uparrow}$ term is almost unaffected by disorder; in contrast, $K_{\downarrow\downarrow}$ is strongly reduced. We note that although band broadening (and thereby MCA) can depend on chemical short-range order, the latter is expected to be negligible in the present alloy with chemically similar constituents.

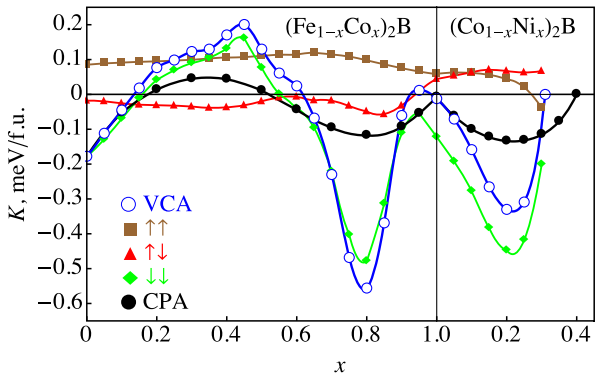

FIG. 3 (color online). MCA in $(Fe_{1-x}Co_x)_2B$ and $(Co_{1-x}Ni_x)_2B$ alloys calculated within VCA (empty circles) compared with CPA (filled circles). The spin decomposition is given for VCA.

The strongest suppression of MCA can be expected for the "hot spots" appearing when nearly degenerate bands at E_F are split by SOC [14]. A clear example of such bands is seen near the Γ point in Fig. 2(a). The effect of disorder is further illustrated in Fig. 4 showing the spectral function at the Γ point for two orientations of the magnetization at $x = 1$, 0.9, and 0.8, all at $T = 0$. At $x = 1$ there is no disorder, and the sharp bands are fully split by SOC for $\mathbf{M} \| z$. With the addition of Fe, the broadening quickly exceeds the original SOC-induced splitting, and the effect of SOC is strongly suppressed.

Disorder has a similar effect on the mixing of electronic bands of opposite spin by L_+S_- and L_-S_+. Indeed, while in Fig. 2(a) for $T = 0$ the anticrossings with the majority-spin bands are clearly visible, in Fig. 2(b), for $T/T_C = 0.7$, they are almost completely suppressed.

We now return to the analysis of the anomalous temperature dependence of K. We expect that these anomalies come from the effects of thermal spin fluctuations on the electronic structure beyond a simple averaging over spin directions. As we saw in Fig. 2, there are two such effects in $(Fe_{1-x}Co_x)_2B$: reduction of the exchange splitting Δ, and band broadening. The reduction of Δ shifts the minority-spin bands downward relative to E_F, just as the band filling with increasing x does. Band broadening has a stronger effect on the minority-spin states, where E_F lies within the relatively heavy $3d$ bands, and it is particularly important for nearly degenerate bands straddling the Fermi level, as we saw in Fig. 4.

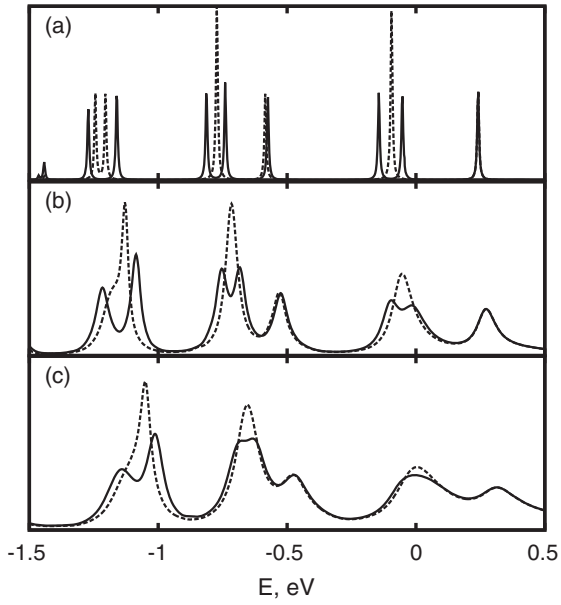

FIG. 4. Spectral functions at the Γ point at (a) $x = 1$, (b) $x = 0.9$, (c) $x = 0.8$. Solid lines: $\mathbf{M} \| z$. Dashed lines: $\mathbf{M} \| x$. A small imaginary part is added to energy to resolve the bands in panel (a).

To understand how these effects lead to the anomalies in $K(T)$, it is convenient to examine two quantities, $K_\uparrow$ and $K_\downarrow$, defined as $K_\sigma = \int^{E_0}(E-E_0)\Delta N_\sigma(E)dE$, where E_0 is the Fermi energy in the absence of SOC, and ΔN_σ is the difference, between $\mathbf{M}\|x$ and $\mathbf{M}\|z$, in the partial density of states for spin σ in the global reference frame. Their sum $K_\uparrow + K_\downarrow$ closely approximates K, and their analysis can help identify the contributions of different bands to K, particularly in combination with reciprocal-space resolution [16,25].

Figure 5(a) shows the temperature dependence of K_σ in Fe_2B. Since the spin-mixing contribution $K_{\uparrow\downarrow}$ here is small (Fig. 3), $K_\uparrow$ and $K_\downarrow$ provide information similar to $K_{\uparrow\uparrow}$ and $K_{\downarrow\downarrow}$ at $T=0$ while retaining clear meaning at finite temperature [25]. We see that $K_\downarrow$ decreases quickly with increasing T. This happens because the downward shift and broadening of the minority-spin bands strongly suppress the negative minority-spin contribution to K. In contrast, the initial increase in $K_\uparrow$ mirrors the upward slope of $K_{\uparrow\uparrow}(x,0)$ as a function of x [16], which occurs as the majority-spin bands shift upward relative to E_F with decreasing Δ. At elevated temperatures the majority-spin contribution becomes dominant, and K undergoes an anomalous sign change, i.e., a spin-reorientation transition.

At the Co-rich end the situation is complicated by the presence of large contributions of opposite sign that come from the minority-spin states in different regions of the Brillouin zone [16]. Near the Γ point there is a large positive contribution from the degenerate bands that are mixed by L_z. There is also a large negative contribution from the mixing of minority-spin bands of opposite parity with respect to σ_z reflection, which is distributed over the whole Brillouin zone. To help resolve these contributions, Fig. 5(b) for $(Fe_{0.05}Co_{0.95})_2B$ shows, in addition to K_σ, the total positive (K_σ^+) and negative (K_σ^-) contributions to K_σ, which were sorted by wave vector. Figure 6 displays $\mathbf{k}$-resolved $K_\downarrow$ on the ΓMX plane at $T=0$ and $T/T_C = 0.7$. The bright red ring around the Γ point in Fig. 6 is the hot spot coming from the two nearly degenerate bands that are split by SOC [see Figs. 2(a) and 4].

As seen in Fig. 6, thermal spin disorder strongly suppresses the hot spot observed at $T=0$: it is strongly washed out at $T/T_C = 0.7$, while the contributions from other regions decline almost homogeneously. This effect is similar to that of chemical disorder (Fig. 4). As a result, $K_\downarrow^+$ declines faster compared to other contributions shown in Fig. 5(b), and the negative value of K grows anomalously with T.

Interestingly, while in VCA the maximum in $K(x,0)$ with respect to band filling occurs near $x = 0.95$ (Fig. 3), in CPA there is a cusped maximum *exactly* in Co_2B. The latter is due to the fact that the bands are broadened by disorder with any admixture, reducing the positive contribution from the hot spots. This dominant effect of disorder explains why, as noted above, the anomalous $K(T)$ dependence at $x \geq 0.9$ is opposite to the trend expected from increasing x, which holds at other concentrations. In Co_2B, where the positive contribution is at its maximum, both band broadening and decreasing Δ contribute to the anomalous decrease in $K(T)$, as the nearly degenerate bands broaden and sink below E_F.

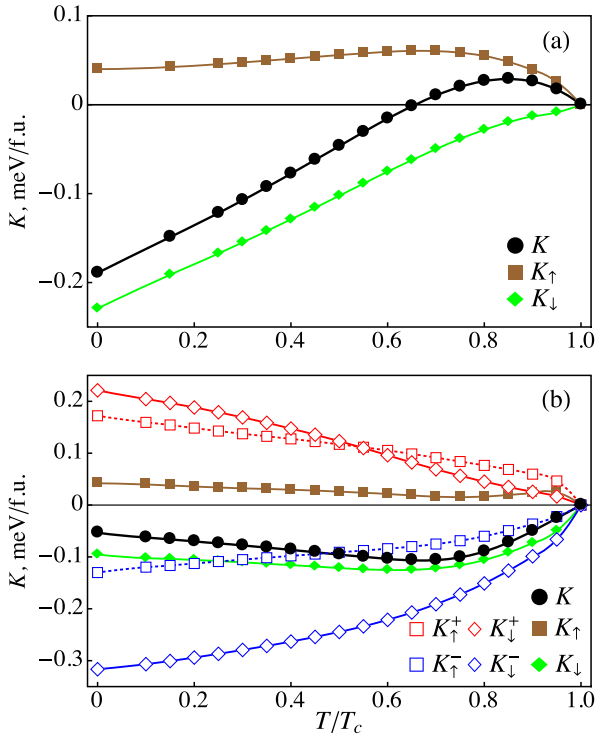

FIG. 5 (color online). Contributions to K in (a) Fe_2B and (b) $(Fe_{0.05}Co_{0.95})_2B$ from different spins ($K_\uparrow$ and $K_\downarrow$). K_σ^+ and K_σ^- in panel (b): total positive and negative contributions to K_σ coming from different $\mathbf{k}$ points. (Dotted lines show $K_\uparrow^+$, $K_\uparrow^-$.)

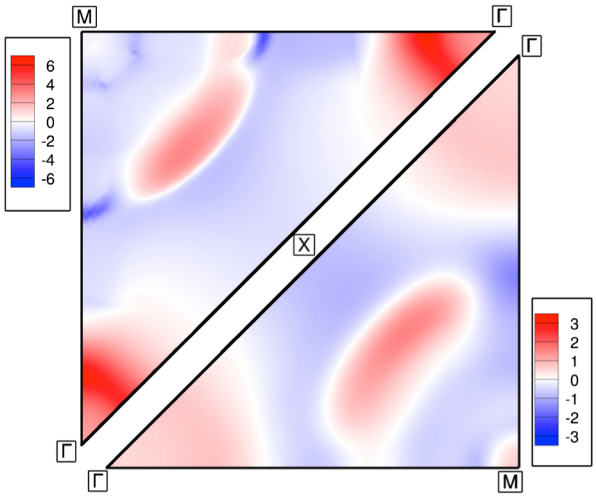

FIG. 6 (color online). Wave vector-resolved $K_\downarrow$ (units of meVa_0^3, where a_0 is the Bohr radius) on the ΓMX plane in the $(Fe_{0.05}Co_{0.95})_2B$ alloy at $T=0$ (upper left) and $T/T_C = 0.7$ (lower right).

In conclusion, we found that the anomalous temperature dependence of MCA in $(Fe_{1-x}Co_x)_2B$ alloys is due to the changes in the electronic structure induced by spin fluctuations. This unconventional mechanism can be harnessed in applications where temperature-independent or increasing MCA is required.

The work at UNL was supported by the National Science Foundation through Grant No. DMR-1308751 and performed utilizing the Holland Computing Center of the University of Nebraska. Work at Ames Laboratory was supported in part by the Critical Materials Institute, an Energy Innovation Hub funded by the U.S. DOE and by the Office of Basic Energy Science, Division of Materials Science and Engineering. Ames Laboratory is operated for the U.S. DOE by Iowa State University under Contract No. DE-AC02-07CH11358.

[1] J. Stohr and H. Siegmann, in *Magnetism: From Fundamentals to Nanoscale Dynamics* (Springer, Berlin, 2006), p. 805.
[2] L. H. Lewis and F. Jiménez-Villacorta, Metall. Mater. Trans. A **44**, 2 (2013).
[3] M. H. Kryder, E. C. Gage, T. W. McDaniel, W. A. Challener, R. E. Rottmayer, G. Ju, Y.-T. Hsia, and M. F. Erden, Proc. IEEE **96**, 1810 (2008).
[4] H. B. Callen and E. Callen, J. Phys. Chem. Solids **27**, 1271 (1966).
[5] W. J. Carr, Phys. Rev. B **109**, 1971 (1958).
[6] V. P. Antropov, V. N. Antonov, L. V. Bekenov, A. Kutepov, and G. Kotliar, Phys. Rev. B **90**, 054404 (2014).
[7] M. Colarieti-Tosti, T. Burkert, O. Eriksson, L. Nordström, and M. S. S. Brooks, Phys. Rev. B **72**, 094423 (2005).
[8] J. F. Herbst, Rev. Mod. Phys. **63**, 819 (1991).
[9] D. P. Pappas, K.-P. Kämper, and H. Hopster, Phys. Rev. Lett. **64**, 3179 (1990).
[10] C. A. F. Vaz, J. A. C. Bland, and G. Lauhoff, Rep. Prog. Phys. **71**, 056501 (2008).
[11] Á. Buruzs, P. Weinberger, L. Szunyogh, L. Udvardi, P. I. Chleboun, A. M. Fischer, and J. B. Staunton, Phys. Rev. B **76**, 064417 (2007).
[12] S. Okamoto, N. Kikuchi, O. Kitakami, T. Miyazaki, and Y. Shimada, and K. Fukamichi, Phys. Rev. B **66**, 024413 (2002).
[13] O. N. Mryasov, U. Nowak, K. Y. Guslienko, and R. W. Chantrell, Europhys. Lett. **69**, 805 (2005).
[14] E. I. Kondorskiĭ and E. Straube, Zh. Eksp. Teor. Fiz. **63**, 356 (1972) [Sov. Phys. JETP **36**, 188 (1973)].
[15] A. Iga, Jpn. J. Appl. Phys. **9**, 415 (1970).
[16] K. D. Belashchenko, L. Ke, M. Däne, L. X. Benedict, T. N. Lamichhane, V. Tarfour, A. Jesche, S. L. Bud'ko, P. C. Canfield, and V. P. Antropov, Appl. Phys. Lett. **106**, 062408 (2015).
[17] I. Turek, V. Drchal, J. Kudrnovský, M. Sob, and P. Weinberger, *Electronic Structure of Disordered Alloys, Surfaces, and Interfaces* (Kluwer, Boston, 1997).
[18] I. Turek, V. Drchal, and J. Kudrnovský, Philos. Mag. **88**, 2787 (2008).
[19] T. Oguchi, K. Terakura, and N. Hamada, J. Phys. F **13**, 145 (1983).
[20] B. L. Györffy, A. J. Pindor, J. B. Staunton, G. M. Stocks, and H. Winter, J. Phys. F **15**, 1337 (1985).
[21] J. B. Staunton, S. Ostanin, S. S. A. Razee, B. L. Gyorffy, L. Szunyogh, B. Ginatempo, and E. Bruno, Phys. Rev. Lett. **93**, 257204 (2004).
[22] J. B. Staunton, L. Szunyogh, A. Buruzs, B. L. Gyorffy, S. Ostanin, and L. Udvardi, Phys. Rev. B **74**, 144411 (2006).
[23] M. Matsumoto, R. Banerjee, and J. B. Staunton, Phys. Rev. B **90**, 054421 (2014).
[24] B. S. Pujari, P. Larson, V. P. Antropov, and K. D. Belashchenko, Phys. Rev. Lett. **115**, 057203 (2015).
[25] See Supplemental Material at http://link.aps.org/supplemental/10.1103/PhysRevLett.115.217201, which includes Refs. [26–35], for technical details and additional figures.
[26] A. I. Liechtenstein, M. I. Katsnelson, V. P. Antropov, and V. A. Gubanov, J. Magn. Magn. Mater. **67**, 65 (1987).
[27] K. Chen, A. M. Ferrenberg, and D. P. Landau, Phys. Rev. B **48**, 3249 (1993).
[28] V. P. Antropov, M. I. Katsnelson, and A. I. Liechtenstein, Physica (Amsterdam) **237–238B**, 336 (1997).
[29] V. P. Antropov, J. Magn. Magn. Mater. **262**, L192 (2003).
[30] L. Takacs, M. C. Cadeville, and I. Vincze, J. Phys. F **5**, 800 (1975).
[31] O. K. Andersen, Phys. Rev. B **12**, 3060 (1975).
[32] D. D. Koelling and B. N. Harmon, J. Phys. C **10**, 3107 (1977).
[33] I. V. Solovyev, P. H. Dederichs, and I. Mertig, Phys. Rev. B **52**, 13419 (1995).
[34] V. P. Antropov, L. Ke, and D. Aberg, Solid State Commun. **194**, 35 (2014).
[35] A. Edström, M. Werwiński, J. Rusz, O. Eriksson, K. P. Skokov, I. A. Radulov, S. Ener, M. D. Kuz'min, J. Hong, M. Fries, D. Yu. Karpenkov, O. Gutfleisch, P. Toson, and J. Fidler, arXiv:1502.05916.
[36] T. Moriya, *Spin Fluctuations in Itinerant Electron Magnetism* (Springer, Berlin, 1985).
[37] V. P. Antropov and A. Solontsov, J. Appl. Phys. **109**, 07E116 (2011).
[38] The scaling of the exchange-correlation field in CPA is used only for Co. In VCA calculations the scaling factor is interpolated, similar to the nuclear charge.
[39] K. H. J. Buschow, in *Boron and Refractory Borides*, edited by V. I. Matkovich (Springer, Berlin, 1977).
[40] I. Turek, J. Kudrnovský, and K. Carva, Phys. Rev. B **86**, 174430 (2012).